



Landscape structure model based estimation of the wind erosion risk in Brandenburg, Germany

Roger Funk^{*}, Lidia Völker, Detlef Deumlich

Leibniz Centre for Agricultural Landscape Research, Research Area 1 "Landscape Functioning", Eberswalder Str. 84, Müncheberg 15374, Germany

ARTICLE INFO

Keywords:

Wind erosion risk
Landscape structure model
Laser scanning
Landscape element height
Wind shadowing

ABSTRACT

The paper presents the development, adaptive improvement and use of the method to estimate the wind erosion risk in Germany for Cross Compliance (CC) regulations, based on the German standard DIN19706. It is illustrated by the example of the Federal State of Brandenburg. A landscape structure model was developed which calculates the sheltering effects of landscape elements. Basic inputs are the heights of all landscape elements and the frequencies and directions of erosive winds. In combination with the soil map of erodibility the wind erosion risk is derived in a high spatial resolution according to the CC requirements. In addition to improving the input data in terms of its spatial resolution by using air-borne laser scanning data, an innovative approach is presented which derives the sheltered areas behind landscape elements from the transport capacities of wind speeds above a threshold. Thus, our analysis represents one of the most comprehensive wind erosion assessment of cropland that can be used for landscape structure assessment well beyond CC use. The derivation of effective protection zones from the frequencies of erosive winds when critical thresholds are adjusted represents an innovative approach that provides an objective and transferable assessment of wind protection of landscape features in different wind regimes.

Introduction

Wind erosion is a serious soil degradation problem on agriculturally used land worldwide, mainly related to arid and semi-arid regions (Reich et al., 2001; Borelli et al., 2014). In the sub-humid climate of Northern Germany wind erosion is a seasonal threat especially in the spring months and increasingly in late summer, when the fields are bare and freshly prepared for the following winter crops (Funk & Reuter 2006). Furthermore, aspects of climate change and its particular impacts on wind erosion are becoming important. Recent studies predict longer dry spells, more heat waves and higher wind speeds, which will intensify the wind erosion problem in the future, on the one hand by increasing the intensity and on the other hand by extending it in time (Zolina et al., 2013; Brune, 2016; Gericke et al. 2019). So, short- and long-term effects of wind erosion require specific attention, as they are associated with current management practices and long-term soil and climate changes.

Wind erosion contributes to a gradual decrease of soil fertility on agriculturally used fields, especially by sorting processes of the mixed-grained soils (Goossens & Gross, 2002; Funk et al., 2004a; Bach, 2008; Borelli et al., 2017; Nerger et al., 2017). Fine particles and soil organic

matter (SOM) are removed predominantly and transported as suspension fraction over great distances. The coarser particles of the saltation fraction remain close to the ground and are deposited on the field or at the field boundary. This material is generally characterized by a uniform grain size, dominated by the medium sand fraction (particle diameters between 100 and 630 μm), and the loss of organic material, already indicated in the field site by a lighter colour of the deposits compared to the original soil. In contrast, the suspension fraction is enriched in organic material, nutrients and chemical agents, responsible for additional problems in adjacent or remote, natural or urban areas (Goossens, 2004; Funk & Reuter, 2006; Hoffmann et al., 2008; Hoffmann et al., 2015; Mendez et al., 2017). Enrichment ratios of SOM in the suspension fraction measured in heights above 1 m were always several times above the corresponding concentrations of the original soil (Sterk et al. 1996; Li et al., 2007; Webb et al., 2012; Iturri et al. 2017).

Wind erosion affects traffic safety by its local and sudden occurrence and the released dust in the PM_{10} - and $\text{PM}_{2.5}$ -fractions contributes to air pollution in urban areas (UBA, 2017; Li et al., 2018). Dust from arable land has also impact on atmospheric processes by reflecting and absorbing radiation. Particles of the aerosol sizes ($<20 \mu\text{m}$ in diameter)

^{*} Corresponding author.

E-mail address: rfunk@zalf.de (R. Funk).

<https://doi.org/10.1016/j.aeolia.2023.100878>

Received 4 November 2022; Received in revised form 23 May 2023; Accepted 24 May 2023

Available online 7 June 2023

1875-9637/© 2023 The Author(s). Published by Elsevier B.V. This is an open access article under the CC BY license (<http://creativecommons.org/licenses/by/4.0/>).

initiate the droplet freezing in mixed-phase clouds and have shown a 10-time higher ice nucleation efficiency than desert dust (Conen and Leifeld, 2014; Steinke et al., 2016). Released dust particles of soils are also a favoured transport medium for microbes, which are soil-borne or added by organic fertilizers (Giongo et al., 2013; Favet et al., 2013; McEachran et al., 2015; Münch et al., 2020).

The extent of soils susceptible to wind erosion in the North-Eastern part of Germany is considerable, with about 60 per cent of the arable land in the Federal State of Mecklenburg-Western Pomerania (MVP) and 40 per cent in the Federal State of Brandenburg (BRB), predominantly soils of sandy texture (MLUK, 2021; LUGV, 2016; Funk et al. 2004b). The combination of large fields with high wind velocities close to the coast line of the Baltic Sea in MVP, and dry climatic conditions in BRB are further favouring factors for wind erosion in this region. The main season for wind erosion is spring, when the temperature and air pressure differences between the Atlantic and the continent are responsible for high wind velocities, and the fields for summer crops are bare and fine structured due to seedbed preparations. Especially fields grown with maize are endangered, because the slow germination, the wide row distances and the slim silhouette of the crop maintain the wind erosion risk for a long period of time (Funk & Engel 2015). The repeated occurrence of wind erosion events disturbing the public in north-eastern Germany also always initiates the discussion of whether the area is adequately equipped with windbreaks.

On the other hand, both Federal States MVP and BRB are already characterized by a very diverse landscape structure, including forests, alley trees, hedges, small groves and habitats, which are obstacles for the surface wind and having a protective effect by decreasing the local wind velocity, extracting momentum, and, if related to a specific field area, reducing the wind erosion risk finally (Frielinghaus et al. 2002a; Frielinghaus et al. 2002b; Chappell & Webb 2016; Baker et al. 2021).

Estimations of the wind erosion risk for larger areas are mainly based on soil data (Borelli et al., 2014; Borelli et al. 2016) and the spatial variability of the surface wind velocity as influenced by orography or extended uniform landscape patterns, as forests, grassland or arable land (Pásztor et al., 2016; Troen & Petersen, 1989). The effect of vegetation on the wind field is included as displacement height and aerodynamic roughness length, but attributed to the place of its presence (Funk & Reuter, 2006; Borelli et al., 2015). Thereby, the wind reducing effect of any landscape element is much vaster and may influence leeward distances up to the 40-fold of its height (Hagen et al., 1981; van Eimern, 1964; Vigiak et al. 2003). Wind velocity and radiation are affected primarily, which again have impact on temperature, dew formation, evaporation and soil moisture in these zones influencing wind erosion susceptibility additionally (Nägeli, 1941; Illner, 1956; Schmidt et al. 2019). Approaches that include already the shadowing effect of roughness elements are available, and have been developed by Chappell and Heritage (2007) and were field tested by Ziegler et al. (2020). Based on the work of Elliot (1958), Marshall (1971) and Raupach (1992), they use illumination and shadow to estimate the effects of roughness elements on aerodynamic resistance and flow separation. Here, the influence of the roughness elements on the flow is in the main focus, only one direction is considered and a number of parameters describing size, shape and distribution of the elements are required.

The implementation of the Cross Compliance (CC) regulations for soil protection in 2008 by the European Commission resulted in the demand to classify the wind erosion risk on agricultural used areas in Germany nationwide. A spatial high precise method was needed, adequate to the spatial accuracy of the Digital Field Block Cadastre (DFBK, EC 1593/2000), where a minimum accuracy at least equivalent to a scale of 1:10,000 is demanded. Data sets and validation principles should be uniformly applicable to guaranty a fair and comparable procedure between all farmers. As the classification is also linked to adaptation measures of, and direct payments to the farmers, this method development became a very sensitive, critically observed topic from all sides. The implementation of the CC regulations also required a

justiciable base, which is given in Germany only by laws or standards. Therefore the classification has been based on the standard “Soil quality – Determination of the soil exposure risk from wind erosion” (DIN 19706 Din (2004)), where the authors were also involved in the development. These needs will remain in the future with the introduction of the new EU CAP rules in 2023, where the various effects of windbreak hedges, such as increasing biodiversity or influencing the microclimate will be on the main focus.

Data maintenance and updating were essential parts of the annual calculation of the wind erosion risk assessment for CC in the first years of application (start: 2008) to ensure acceptance by the farmers and avoid later objections. This approach was developed in close cooperation with the regional authorities of Schleswig-Holstein, Lower Saxony and Mecklenburg-Western Pomerania, where equivalent approaches are in use. In this paper, we present the approach exemplarily for the Federal State of Brandenburg (BRB) for which we were responsible.

Among the administrative requirements of the study, the scientific aim was to provide and develop a landscape structure model, which is based on process-orientated classifications and taking into account all relevant parameters influencing site-specific wind erosion with the best available spatial resolution and state-of-the art technology.

Materials and methods

The German standard DIN 19706, “soil quality – Determination of the soil exposure risk from wind erosion”

This standard provides a simple determination scheme for deriving the wind erosion risk stepwise (Fig. 1). For the purposes of CC, the DIN 19706 is not applied in its entirety, but only for the determination of the site-dependent erosion risk. Here, mainly the stable factors are considered, such as the soil type, the average wind velocity as well as the landscape structure. Therefore, in deviation from the scheme shown in Fig. 1, step 3 that evaluates the crop types or crop rotations is not included. Since it could be exchanged with step 4 for the evaluation of the landscape structure anyway, there is no different evaluation up to this point.

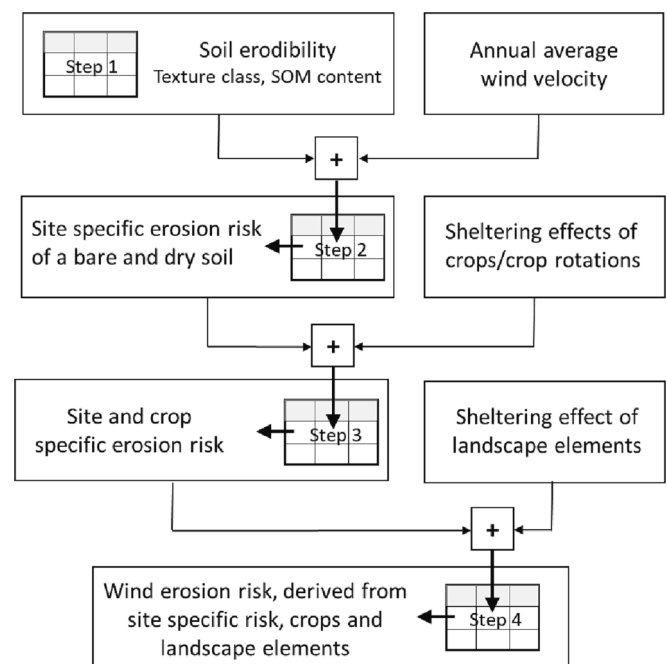


Fig. 1. Scheme of the determination of the wind erosion risk with the DIN 19706.

Considered area

The considered area includes the Federal State of Brandenburg (BRB) and the periphery of the included capital Berlin, covering together an area of about 30,000 km². The methodology is presented using the district Maerkisch-Oderland (MOL) for better illustration. The soils and the surface structure are the result of the last glaciation (Weichsel glacial stage) about 20,000 years ago, with the typical glacial sequence in northeast-southwest direction of ground and end moraines, outwash plains and dunes (De Boer 1992; [Stackebrandt & Franke, 2015](#)). Large areas of the moraines were covered by fluvial and aeolian deposits of sandy texture during the peri- and postglacial periods. These predominant “light” soils are particularly susceptible to wind erosion ([Fig. 2](#)). In addition to these mineral substrates, BRB also has extensive peatland areas with very different degrees of degradation.

The climate in BRB is typical for the transition between oceanic and continental influences. The annual average precipitation is 550 mm, the potential evapotranspiration (PET) is 864 mm, and a climatic water deficit (PET > precipitation) is typical for the months April to September. The wind velocity has its maximum between January and April and the highest transport capacity in March, when strong wind velocities often coincide with a dry soil surface.

BRB has about 10,500 km² of forests, which is 36 % of the total area and mainly locates in the areas where the soils limit agricultural production (too dry, too wet, too steep,...). The range of forested areas between the districts of BRB is between 23 and 46 %, depending on the soil quality ([ATKIS 2013](#)).

The area of interest is finally defined by the Digital Field Block Cadastre (DFBK), which contains all agricultural used fields in Vector Data File formats in a GIS ([LGB 2023](#)). The general form of land use is divided into arable land and grassland. The DFBK has a separate layer including a part of the landscape elements in or adjacent to the field blocks.

Compilation of a complete soil map

Soil maps covering the total area of Germany exist on a scale of 1: 200,000. They show the distribution and association of soils and their properties. In BRB the Geological Service derived a use-independent map series on a scale of 1: 300,000. From the basic data of these soil maps, the functions, potentials and hazards of soils can be determined and represented. The soil map BK50 (scale 1: 50,000) is currently the map with the highest resolution, developed in a similar form in the other Federal States. However, the scale is too rough for the requirements of CC, where a spatial resolution of 1: 10,000 was demanded. Therefore, a soil map was composed from digitized soil maps in vector format with the aim to cover the entire area of the Federal State in one map to prevent additional work by later reassignment of changed land uses or data mismatch during the calculation by not assigned grid cells. Since soil maps are primarily related to the area of agriculturally used land, landscape compartments of other land uses were not included. This deficit is being prevented by this compilation. The map is also used to classify the water erosion risk and represents therefore the uniform dataset for erosion risk assessments in BRB. Data were taken from (listing corresponds to ranking – beginning with the highest spatial resolution):

1. The Soil Quality Appraisal (scale 1:10,000), covering mineral soils of agriculturally used areas; share: 48.7 per cent of the total and 96.7 per cent of the arable land area.
2. The Medium-scale Agricultural Site Mapping (MMK, 1:25,000), used to complete the agriculturally used areas not included in 1.), as peatland, church-owned land and changes from other land use types to agricultural use in the last 50 years (forest, settlements, reclaimed mining areas,...); share: 9.23 per cent of the total and 2.3 per cent of the arable land area.

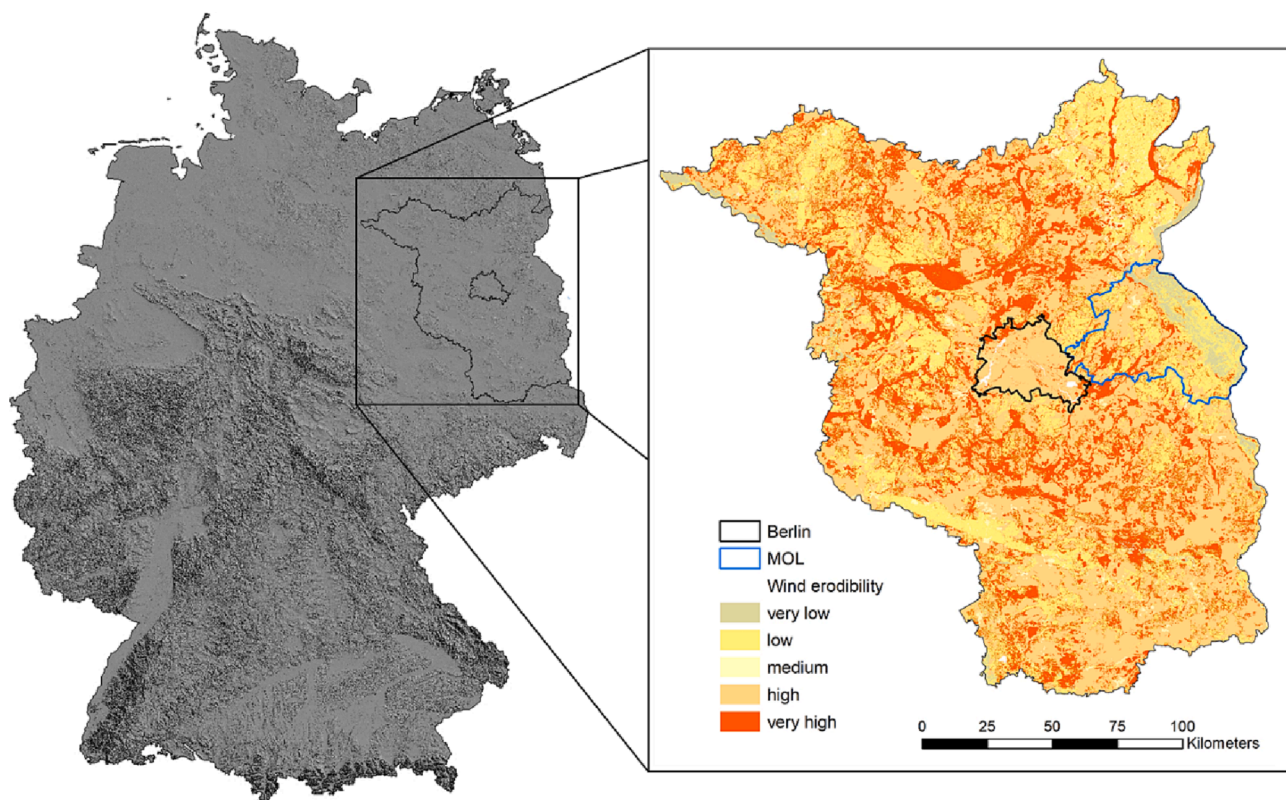


Fig. 2. Location of Brandenburg in Germany and the district Maerkisch-Oderland (MOL) in Brandenburg; right image shows also wind erodibility in Brandenburg derived from soil data (corresponds to step 1 in [Fig. 1](#)).

3. Extrapolation of the MMK to fill still empty pixels as forest areas, settlements, roads, lakes (Böhm et al. 2009); share: 39.6 per cent of the total and 0.83 per cent of the arable land area.
4. Agriculturally used land in Berlin; share: 2.45 per cent of the total and 0.2 per cent of the arable land area.

Based on the mapped soil texture and the SOC content the wind erosion susceptibility was derived in 6 classes (0–5, no risk and very low to very high erodibility) corresponding to step 1 of the DIN 19706. Peat soils were generally classified with the highest erodibility. This follows both the physical basics of the processes, because particles of organic origin are much easier released and transported by wind due to lower density compared to mineral ones, and nature conservation issues as peat soils represent valuable habitats and are carbon enriched. This affects practically only peat soils which are used as arable land. The majority of peat soils used as grassland will not be considered to have an erosion risk in one of the following classification steps.

The original vector data were converted into a grid map with a pixel size of 10×10 m resulting in >304 million pixels.

Wind velocity

The soil map was combined with the map of the annual average wind velocity at 10 m height in Germany, provided in a 200 m grid by the German Weather Service (Fig. 3 right map, DWD, 2004) and resampled for our purpose in a 10×10 m grid too. These wind data show a strong gradient from the coast lines of North and Baltic Sea to the inlands, but not in BRB. The annual average wind velocity (\bar{u}) is more homogeneous and between 2 and 5 ms^{-1} , only slightly modified by the even terrain and the land use patterns. The variability of the wind velocity data reflect primarily land use pattern in BRB (forest or agriculture) (ATKIS 2013; DWD, 2018; CLC, 2018). The annual average wind velocity is used in the classification scheme of the DIN 19706 to upgrade or downgrade erosion risk classes (step 2 in Fig. 1). The classes were increased for wind velocities $>6 \text{ ms}^{-1}$ and decreased for $<3 \text{ ms}^{-1}$, in steps of ± 1 risk class for a difference of $\pm 1 \text{ ms}^{-1}$.

Compilation of a complete landscape structure map

Derivation from maps and other sources

The arrangement, density and height of each landscape element affects the susceptibility to wind erosion by influencing the spatial variability of wind speeds. Thus, information about the location and the properties of all landscape elements, in its entirety the landscape structure, is necessary. In the end, it is particularly important for our approach that each landscape element is assigned a corresponding height since the sheltering effect is expressed as manifold of it.

A landscape structure map was composed using the following different vector data sources, which are available in Brandenburg:

1. Biotope Type Map, area-wide map containing about 650,000 landscape elements in >2500 detailed described classes, origin: interpretation of Colour-Infrared (CIR) aerial images from 2009 and homogenized and updated biotope type data from 1991 to 1993 (scale: 1: 10,000, available from MLUK 2009).
2. Additions from the “Landscape Elements” layer of the Digital Field Block Cadastre (DFBK), containing 130,000 elements located on or adjacent to agriculturally used field blocks, as hedges, solitary trees, cattle holes, stone heaps, and others; origin: digital aerial ortho-photos (scale 1: 2,500, available from LGB 2023).
3. Additions and corrections by the County field block surveyors, at the starting phase annual update of added or removed landscape elements, (hedges, solitary or groves of trees, farm buildings, stables, ...), and corrections of elements from 1. and 2. by measured heights and dimensions directly at the field site.

Height values were attributed to each landscape element depending on the described features in the Biotope and Land Use Maps and the DFBK, in 10 classes from arable land with 0 m to forest with 20 m height (Table 1). The following height values were assigned: 0, 1, 2, 3, 5, 7, 10, 12, 15 and 20 m. In case of presence in both maps the higher value was chosen. All data were combined in one map and converted from vector data to grid data in a 3×3 m raster with 3,375 million pixels. This finer

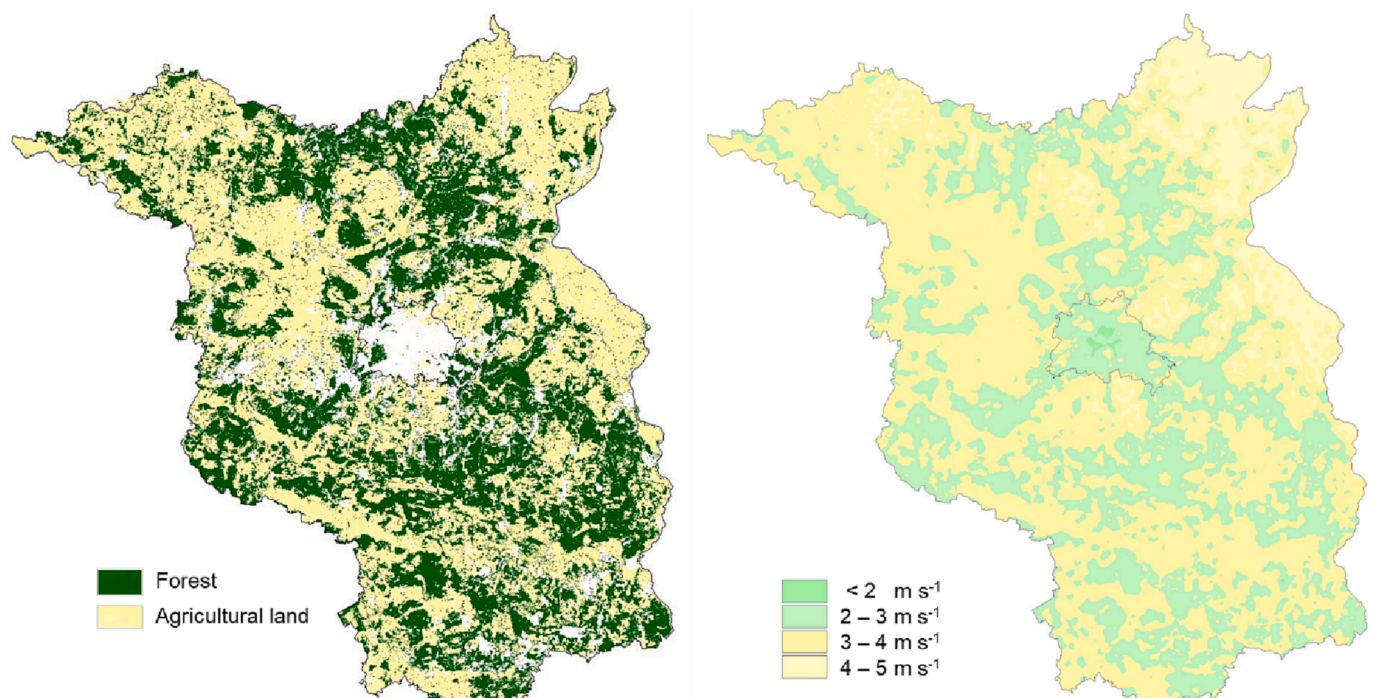


Fig. 3. Main land use in Brandenburg based on ATKIS data (left), and annual average wind velocity in 10 m height based on data from the German Weather Service (DWD); (right: includes already DIN 19706 classification: green – wind erosion risk will be reduced, yellow – wind erosion risk remains as it is).

Table 1

Summarized classes of landscape elements and assigned heights (as height values were assigned: 0, 1, 2, 3, 5, 7, 10, 12, 15 and 20 m).

Landscape element classes	Height (m)
Agriculturally used land, standing waters	0
Running waters with vegetation, swamps, peatland	1
Forb stands, grasslands, field margins, stone walls,	1
Shrubby heaths, coniferous bushes	1 ... 5
Deciduous bushes, hedgerows, alleys	1 ... 20
Woods and forests, orchards	5 ... 20
Green areas, open spaces	2 ... 10
Settlements, traffic facilities	1 ... 10

resolution became necessary in order to represent also the shelter by LE with the height of 1 m. Since the protection areas are designated in multiples of the height, the shelter of protection zone 5 close to the LE with a length of 5 m shown in Fig. 6 are otherwise only partially representable with a 10×10 m grid.

Derivation of the landscape structure from laser scanning

In the recent past new technologies were used to measure and map the surface of the earth with high accuracy based on Radar or Lidar technology (Flood, 2001). In BRB an airborne laser scanning campaign was finished in 2018, covering in the meantime the entire area with a resolution of 1 m and a height accuracy of +/- 50 cm (LGB, 2020). We therefore decided to use this new database for the derivation of height data. The laser scanning resulted in two layers, the Digital Surface model (DSM), including everything with a certain height, and the derived Digital Elevation Model (DEM), representing the land surface after eliminating all landscape elements as buildings or vegetation. The height of any landscape element can be received easily by subtracting the DEM from the DSM. Because topography is also eliminated in this way the new layer includes only the measured landscape elements on a flat surface, comparable with the elements in the landscape structure map described before. Additionally, all height values inside of agricultural land were cleared and set to zero using the structures of the DFBK, because hay bales, vehicles, stacks or temporary silos left in the fields were also measured by the laser scanning during the overflight. As a compromise between accuracy and calculation time we decided to set the cell size of this new layer to 2×2 m (Fig. 4, right).

Determination of the sheltering effect of landscape structure against wind erosion

Previous approach

The wind reducing effect in front and behind any landscape structure element depends on its height and its density (or their opposite equivalent – the porosity). The decrease in wind speed behind hedges or other windbreaks is well studied and shows a drastic decrease on the leeward site at first, which then gradually increases back to the original value with increasing distance. One of the few mathematical descriptions of this curve can be found in the WEPS model, which also includes porosity as an input in addition to height (Eq. (1); Fig. 5). (Hagen and Fox, 2020; USDA-ARS, 2020). Because the considered period for assessing the wind erosion risk is from March to May, where trees and shrubs are still without leaves at the beginning and fully leafy towards the end, we set a porosity of 40% to cover the complete time appropriately.

$$fu = 1 - \exp(-m \cdot x^2) + n \cdot \exp(-0.003(x + s)^t) \tag{1}$$

where *fu* wind reduction factor

x distance from the structure element in multiples of height.

The coefficients *m*, *n*, *s* and *t* depend on porosity (*p*) and are calculated as follows

$$m = 0.008 - 0.17p + 0.17p^{1.05} \tag{2}$$

$$n = 1.35 \exp(-0.5p^{0.2}) \tag{3}$$

$$s = 10(1 - 0.5p) \tag{4}$$

$$t = 3 - p \tag{5}$$

In a Geographic Information System (GIS) the sheltering effect of landscape elements on the wind can be displayed by a shadow (of light) in front and behind each element, by equating the distance of the wind speed reduction with that of the shadow. The GIS procedure “Hillsshade” has been used to set virtual shadows around a landscape element differing in length and direction (Fig. 6). The parameter *azimuth* is the direction of the virtual sun and an equivalent to the wind direction. The length of a shadow can be varied by the *altitude* of the illumination, which is determined by the zenith angle of the virtual sun (α). As the DIN 19706 divides the sheltered distances behind a landscape element into five zones, we set five shadows of different lengths for one direction,



Fig. 4. Section of the landscape elements map, left: assigned heights from the biotope mapping; right: measured heights by laser scanning.

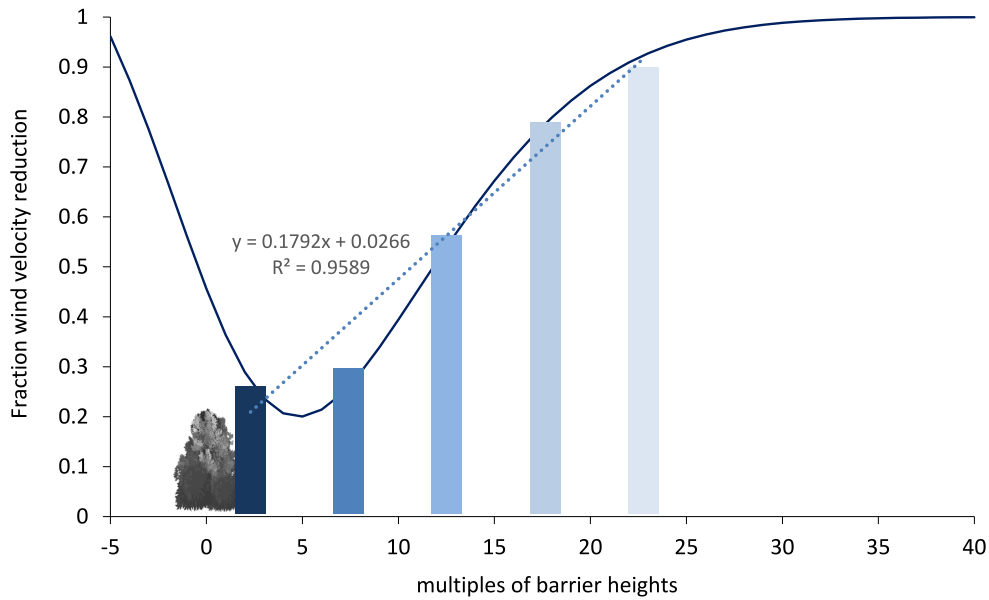


Fig. 5. Wind velocity reduction in front and behind a wind barrier in units of the barrier heights for a porosity of 40% (eq.[1], line); averages of the used classes (bars) and linear regression (dotted line); colours correspond to the protection zones in Fig. 6.

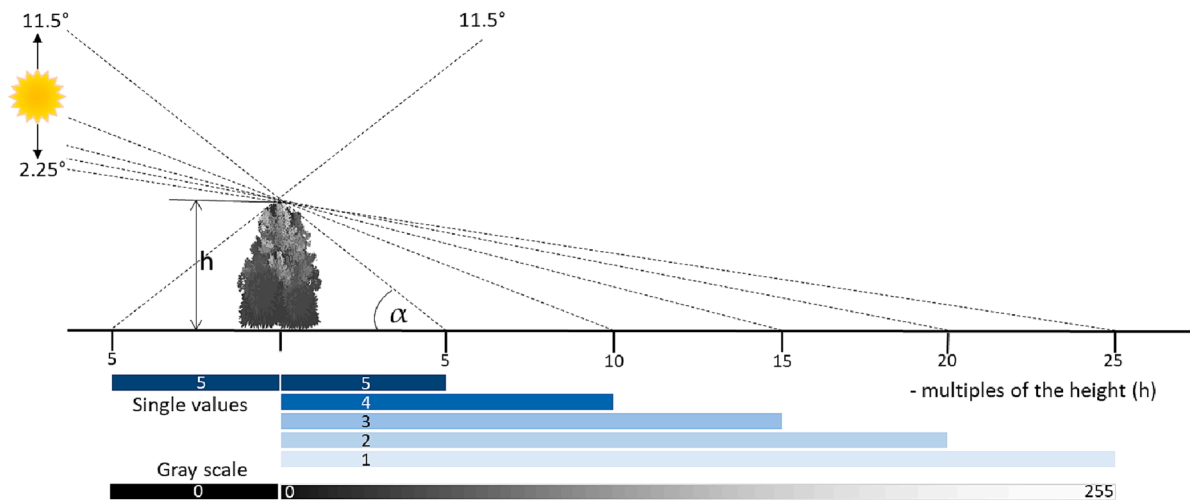


Fig. 6. Illustration of the implementation of the GIS command “hillshade” and “shadow” used to designate protection zones in front and behind landscape elements.

each filled with decreasing numerical values from 5 to 1, representing the decreasing sheltering effect with increasing distance. We used five zenith angles of illumination for one direction, and one for the opposite direction, as well as eight directions (0°, 45°, 90°, ...) to create 48 new layers with shelter of different lengths in the eight directions. All were combined in one final layer by taking the maximum numeric value of each cell. The newly created layers with the calculated protected zones were then transferred back to the 10×10 m grid.

A question during the method development was, how good the protected zones created by the GIS represent the nonlinear relationship between distance from a wind barrier and wind velocity reduction from equation [1]. By averaging the values within the classes made up in steps of 5-fold the height as used in Fig. 6, a linear relation can be derived, which can be considered as sufficiently accurate for our purposes as shown in Fig. 5.

At this point, DIN 19706 ends without a specific consideration of wind directions, which, however, must be taken into account in an evaluation of landscape structures. For BRB, we developed the following procedure: The maximum sheltering distance in each wind direction was

set to the 20-fold of the height by not considering protection zone 1. The reasons for this were: trees in March and April are mostly leafless and there is a high probability of wind speeds above the threshold of 6 m s⁻¹, which will initiate wind erosion already after shorter distances at the leeward side again. The prevailing wind direction has also influence on the effectiveness of a landscape element. Especially linear structures like hedges are more effective if orientated perpendicular to the main wind direction than parallel. This was taken into account by including the frequency of wind velocities above the threshold of 6 m s⁻¹ for each wind direction. The relative frequencies of hourly wind velocities above 6 m s⁻¹ in the months March to May of eight sectors (0°-45°, 46°-90°...) were used as a weighting factor and multiplied with the numerical values of the shadowed cells of the opposite direction (Fig. 7). The wind direction with the highest frequency was given the factor 1, the other directions were weighted accordingly lower. This should not express a lower protection of shelter belts against the other wind directions, but that these sheltered areas are more often affected by the wind from the main wind direction.

The final step in this wind erosion risk estimation is the query of the

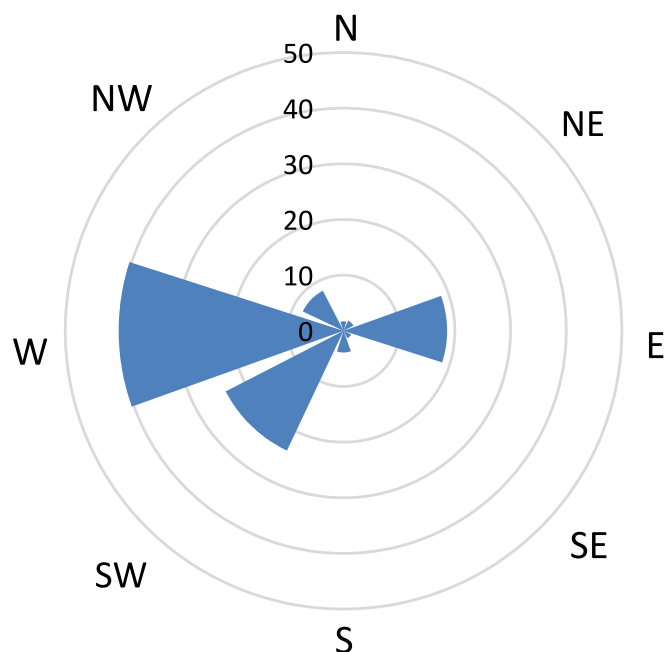


Fig. 7. Relative frequency (%) of wind velocities > 6 m s⁻¹ in the months March – May, classified for eight main wind directions (average of 1991–2000).

risk classes to each field block. It has been determined for Cross Compliance that field blocks with a share of >50 % of its area in the wind erosion risk class “very high” must have protective measures in place.

New approach – Derivation of the sheltering distance from the transport capacity of the wind

In the new approach, two aspects are considered. One is the increasing transport capacity of the wind by exceeding the threshold in relationship to its frequency of occurrence, and the second one is to derive the protected areas behind a landscape element based on this weighted transport capacity. The first step is shown in Fig. 8, from the

frequency distribution of wind > 6 m s⁻¹ and the corresponding transport capacity of each wind velocity a weighted transport capacity is derived.

The range of influence of a windbreak for wind velocity reduction is often given as 40 times of its height, as shown in Fig. 5. This refers only to the achievement of the initial level. Considering wind velocities that are above the threshold value, these distances are much shorter. Based on the determined threshold wind velocity of 6 m s⁻¹ for the sandy soils in BRB, the effective protection zone can be calculated in relation to the wind velocities above the threshold. Fig. 9 shows the wind velocity reduction around a wind barrier for all wind velocities above the threshold, calculated with using Equation [1] for a porosity of 40%. The numbers between the lines quantify the fraction of the individual wind velocity class (in steps of 1 m s⁻¹) to the total transport capacity. In Table 2 finally the full length, or the effective protection length, based on the transport capacity of all erosive wind velocities is derived. This is for the frequency distribution of all winds > 6 m s⁻¹ in Müncheberg 18.2 times the height of any landscape element. This full length is now completely taken into account for the wind protection (old approach – 20 times the height by omitting protection zone 1). With the soil erodibility, an intersection according to Table 3 takes place and the wind erosion risk is presented accordingly.

Results and discussion

Wind erosion risk in Brandenburg (previous approach)

Based on the described procedure the wind erosion risk has been estimated every year for the arable land in BRB, starting in 2008. Every year each farm/farmer in BRB got a data set containing the landscape elements, the wind shadows and the remaining areas of high erodibility in the field blocks for the CC proposals. The most changes regarding structural elements had to be managed in the first years. Missing hedges were added, heights corrected, gaps closed or demolished buildings removed. Farmer objections were reviewed and facts corrected as necessary. In relation to the total area of BRB these changes were without any influence, but for the affected farms it was relevant, because the CC classification of entire field blocks could be changed. In 2011 this process was completed and the same landscape structure was used for

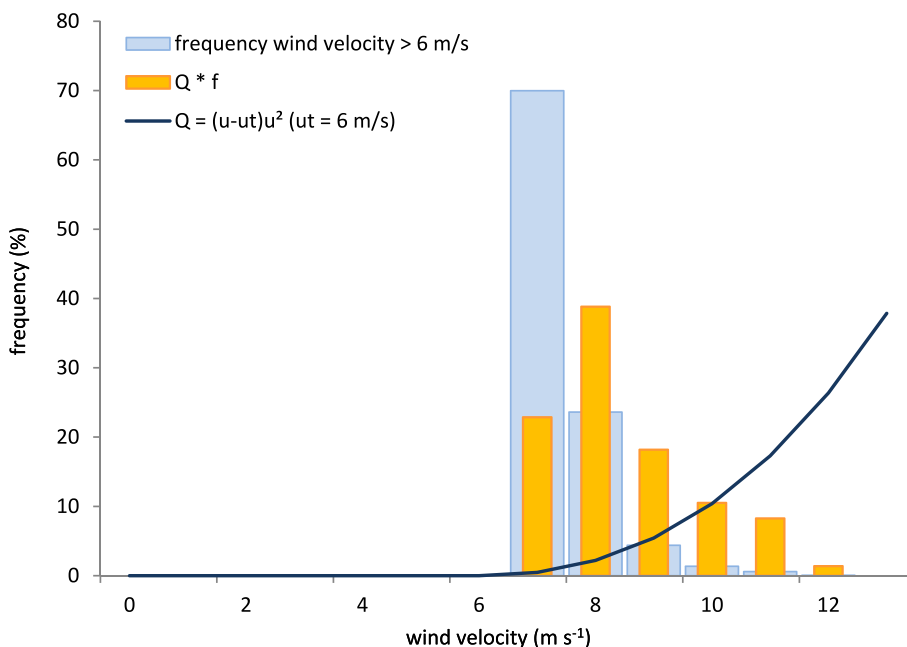


Fig. 8. Frequency of hourly wind velocities above the threshold of 6 m s⁻¹ (light blue bars); transport capacity of the wind based on the relationship $Q = (u-u_t)u^2$ (black line); frequency related transport capacity $Q * f$ (orange bars).

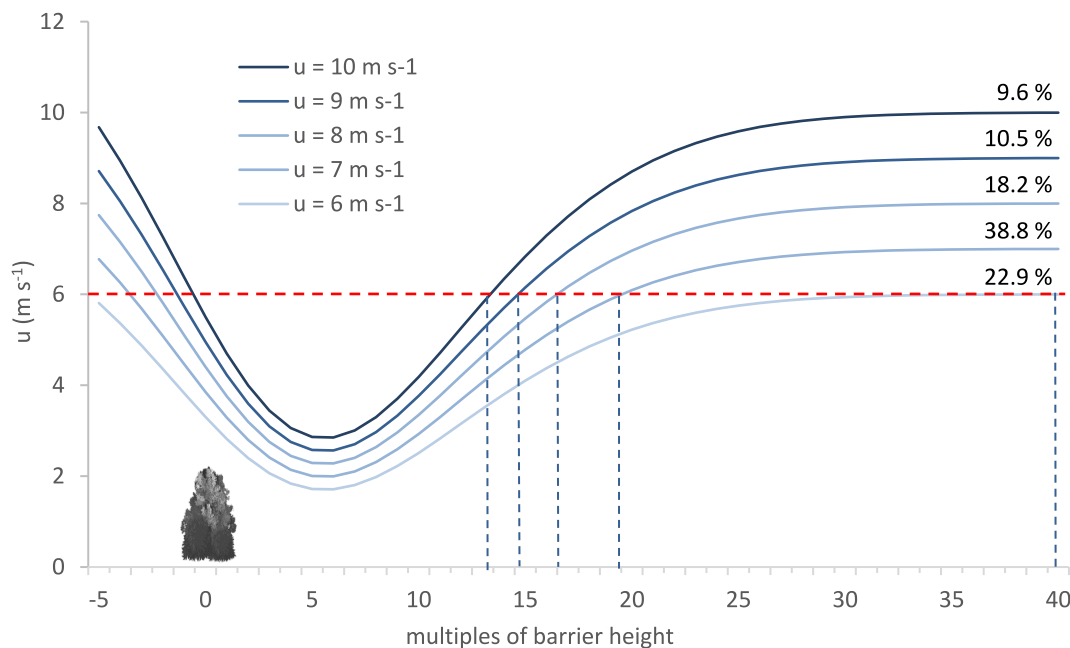


Fig. 9. Wind velocity reduction in front and behind a landscape element for different wind velocities; red dotted line marks the threshold wind velocity for wind erosion on sandy soils, numbers between the curves are the relative transport capacity of each wind velocity level (6–7, 7–8, ... m s⁻¹) for MOL.

Table 2

Derivation of the effective protection zone behind a landscape element, taking into account the transport capacities of all occurring wind velocities above the threshold.

Wind velocity class	class middle in multiples of height (A)	relative transport capacity (%) (B)	A * B Σ/100
6–7 m s ⁻¹	28	22.9	641.2
7–8 m s ⁻¹	17.5	38.8	679.0
8–9 m s ⁻¹	15	18.2	273.0
9–10 m s ⁻¹	12.8	10.5	134.4
> 10 m s ⁻¹	10	9.6	96.0
			18.2

Table 3

Matrix to combine soil erodibility and protection zones.

Soil erodibility	Wind shadowing protection zone					
	5	4	3	2	1	0
No risk 0	0	0	0	0	0	0
Very low 1	0	0	0	0	0	1
Low 2	0	0	0	0	1	2
Medium 3	0	0	0	1	2	3
High 4	0	0	1	2	3	4
Very high 5	0	1	2	3	4	5

the calculations in the following years until it was replaced by the laser scanning in 2020.

The site specific wind erosion risk of a bare and dry soil derived from soil texture and SOM content (step 1 in Fig. 1) is listed in Table 5 (left columns). The classes “high” and “very high” of the entire area in BRB are in total about 70 per cent or 20,000 km² (Fig. 2, right map). That is in accordance with estimations of the Geological Service of BRB, which classifies 67 per cent of the country’s surface into these categories (LGBR 2020). Thus, the extrapolation of MMK maps from agriculturally used land to other areas provides comparable and reasonable results for the derivation of soil erodibility.

Step 2 of the determination scheme includes the spatial differences of the annual averages of wind velocity and results in a considerable decrease of the wind erosion risk. Since topography in BRB is relatively

flat with the highest elevation of 200 m, the forested areas determine the spatial distribution of the annual average wind velocity (Fig. 2). In this step wind velocity reduction and land use as forests affect almost identical proportions of the area. Here it is primarily the on-site effect of the landscape structure in terms of a soil cover. Since forests in BRB are located mostly on areas that are too poor for agriculture, such as sandy cover layers or dunes, the two highest risk classes are affected in particular. The remaining area of arable land is about 10,000 km². Here, 3,800 km² are in the risk classes “high” and “very high”, which is about 37 per cent of the arable land or 12 per cent of the total area of BRB (Table 4, middle columns). The direct effect of wind velocity reduction on the arable land area results in only small changes, about 3.9 per cent of the very high risk class changes to lower classes. For BRB, this step is not mandatory, as a direct dependence between lower wind speeds and forested areas is shown. It is more important near the coast, where higher wind speeds occur area-wide and a strong gradient towards the inland exists. On the contrary, some problems of correct designation of high risk areas resulted from the very large pixel sizes of 200 m of the wind velocity grid, which in some cases extended further into the agricultural areas than the wind shadows calculated in the next step. This led in some cases to a wrong assignment in the risk category of a field block and were solved manually for each detected field block. This step is needed more for reasons of comparability and equal evaluation with the other Federal States than for spatial differentiation within BRB.

In step 4 the landscape elements were included with their wind reducing effects as described in chapter 2.6. Here, we will first refer to the previous version of the analysis, which uses the assigned height values of landscape elements. Including the wind reducing effects of landscape elements, the wind erosion affected area decrease considerably again (Table 4, right columns; Fig. 10). The area in the two highest risk classes decreases from 37 per cent to 18 per cent of the arable land area. There are also great changes in the lower risk classes, with the largest increase to the areas with “none risk”. This drastic change demonstrates the importance of the landscape structure on wind erosion and emphasizes the benefits of shelterbelts.

New approach – Laser scanning of landscape elements

The use of the laser scanning in 2020 changed the data situation

Table 4

Shares of the wind erosion risk classes in BRB derived for the total area (shown in the right map of Fig. 1), for the arable land area (as indicated in the left map of Fig. 2) and the arable land area including the wind reducing effects of landscape elements.

Wind erosion risk	Total area (BRB and Berlin) (Step 1, texture and SOM)		Arable land (BRB and Berlin) (Step 2, incl. land use)		Arable land (BRB and Berlin) (Step 4, incl. wind reduction)		
	km ²	Per cent	km ²	Per cent	km ²	Per cent	Changes (km ²)
None	0.501	0.002	0.389	0.1	2,870.537	27.94	+2,870.148
Very low	713.028	2.34	350.037	3.4	1,229.531	11.97	+879.494
Low	7,584.013	24.91	6,103.559	59.4	3,756.933	36.57	-2,346.626
Medium	658.103	2.16	36.975	0.3	555.447	5.41	+518.472
High	13,556.448	44.53	838.897	7.9	823.119	8.01	-15.778
Very high	7,934.694	26.06	2,959.754	28.9	1,037.237	10.10	-1,922.517
Sum	30,446.788	100.0	10,289.611	100.0	10,272.805	100.0	

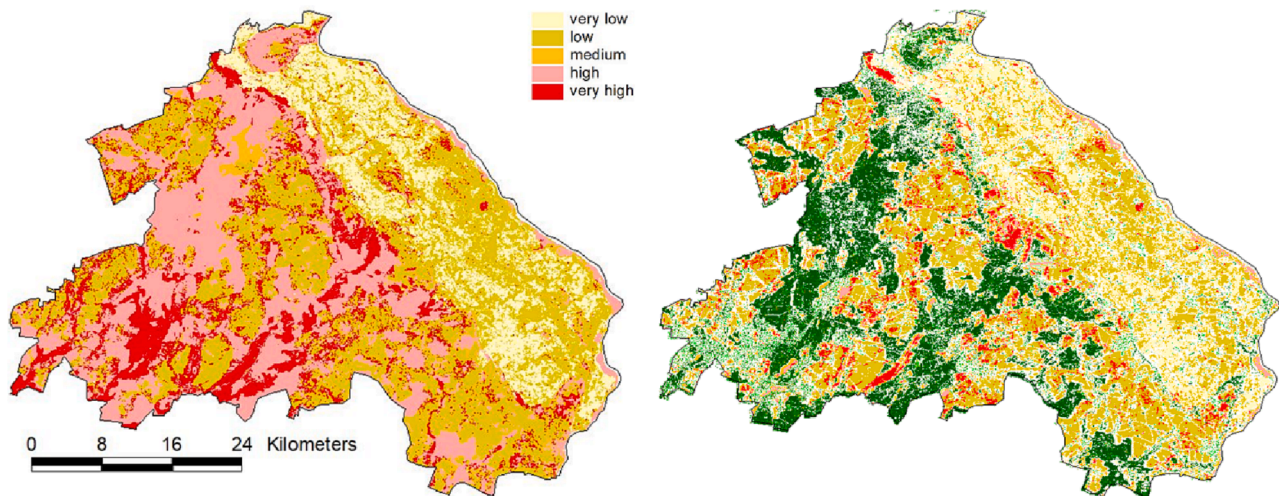


Fig. 10. Wind erosion risk in the county MOL, left: based on soil data, right: including landscape structure and wind reducing effects.

significantly, both in the horizontal and vertical dimensions. Whereas landscape elements in the previous approach were like blocks or walls with discrete values, the laser scan structures are much finer and more divers with rather steady values. There are major shifts and a large number of new distributions in each height class. A comparison between four selected height classes (1, 5, 10 and 20 m) of the assigned landscape elements of the map-derived version and the laser scanning is shown on the example of the district Maerkisch-Oderland (MOL, blue bordered area in Fig. 2). Here is only 23% of the area covered with forests (average BRB 35.5%), so that a relatively larger part of landscape structure elements around the field blocks contributes to the evaluation (Fig. 11, Table 5). There is a better agreement for the higher heights, as evidenced by the shift of the exact fit (red bar) to the centre of the distributions. The height class of 10 m has the largest deviations in both directions. This can be explained by the fact that this height was given predominantly to settlements, but especially here the most different uses and therefore heights can be found (lawns, gardens, streets, houses, church towers, trees...). At the greater heights, which causes longer shadows, an underestimation is evident in the assigned height class of 20 m for the landscape elements of the previous approach.

T 6 shows to what extent the laser scan leads to changes in the heights of the landscape structures. The finer resolution, with the larger part of pixels without a height, does not inevitably lead to poorer protection. This mainly affects the forests, represented in the previous approach as compact blocks, but a uniform distribution is more important for a good protection than a higher density, since the final joining of all shelter zones from all wind directions results in an overlapping. In addition, since there is a significant increase of landscape elements with greater heights and thus longer sheltered distances from the laser scan, it can be assumed that this will compensate the patchiness. The question

here is if the compact structure of the previous approach compensates the lower heights. In Fig. 12 the wind shelter of both approaches are shown. The compact structure of the landscape elements of the previous approach is evident from the very uniform sheltered areas. The protected areas of the laser scan measured heights are much more fragmented, but are often longer.

In MOL, the use of heights from laser scanning of landscape elements halves the area at risk of wind erosion. From formerly 18,740 ha now only 9,615 ha are in the CC-relevant highest erosion risk class. So, it can be concluded that the higher heights dominate over the patchiness.

New approach – Transport capacity derived wind protection lengths

Using the laser scanned heights and the transport capacity derived lengths of wind protection results in an expectable increase of the wind erosion affected area for MOL compared to the previous approach. This is primarily attributable to the shortened maximum lengths of the protection zones, which decrease from the 20-fold to the 18.2-fold of the heights with otherwise identical inputs. Initially there is an increase of the area compared to the previous approach using the laser scan data, from 9,615 ha to 12,114 ha, but the comparison to the baseline situation with the assigned heights brings a reduction of the wind erosion risk area by one third, from 18,740 ha to 12,114 ha. Thus, even in this case, it can be concluded that the greater heights dominate over the patchiness.

Conclusions

The aim of the paper is to show the development and the scientific background of a method used to estimate the wind erosion risk for the Cross Compliance regulations in Germany. The exclusive use of this

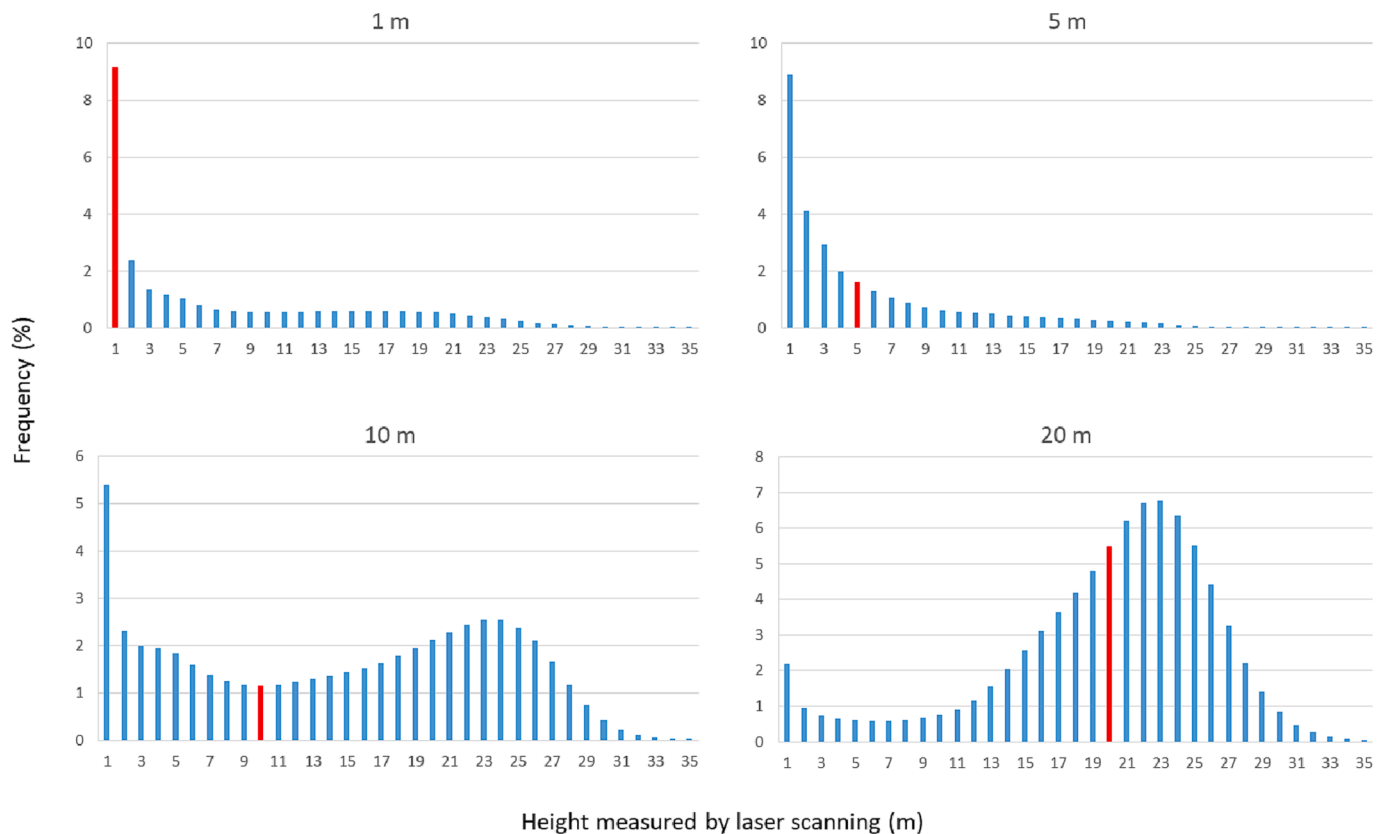


Fig. 11. Frequency distribution of measured heights of landscape elements by laser scanning to the assigned heights (red bars), example of the district Maerkisch-Oderland (MOL).

Table 5
Comparison of assigned and measured heights by laser scanning of the district Maerkisch-Oderland (MOL).

Assigned height (previous approach)	Exact fit to laser scan (%)	Higher height in laser scan (%)	Smaller height in laser scan (%), and part without height (=0 m)
1	9.13	17.2	73.7 (73.7)
5	1.59	9.4	89.04 (71.11)
10	1.15	34.3	64.56 (45.72)
20	5.51	44.8	49.69 (17.32)

method for administrative purposes led to a disconnection to the scientific record keeping, which is hereby made up for. This wind erosion risk assessment is already 14 years in use, so that a very precise detailed knowledge is available, from the administrative overview to the punctual erosion risk on each field block and each landscape structure element at the farm levels. Currently, wind erosion risk for the 30,000 km² of BRB can be determined on a 2×2 m grid.

The study emphasizes the importance of landscape structures on wind erosion, which lead generally to a significant reduction in the risk. Two major improvements have been integrated in the last year: the first concerns the improvement of the input data by the use of airborne laser scanning for the heights of all landscape structural elements of the entire area of BRB, and the second the derivation of the effective protection zones behind landscape structures from the transport capacity of the occurring wind speeds. This leads to a more accurate representation of the processes involved, but also allows a much more flexible application, in which regional, but also seasonal differences can be better taken into account. Our more intuitive decision to limit the maximum protection distance in the previous approach to the 20-fold of the barrier height represents relatively well the more process-related distance of 18.2 times the height, so there will not be too many changes for a

reassessment on this basis.

Even if we consider the landscape structure as a relatively stable element in the evaluation, changes also occurred here over the years. The aerial survey of the entire area of BRB for the DEM already took 10 years, so that the vegetation heights of the areas surveyed first can no longer correspond to the current status in the DOM completely, since trees grow or are also cut down. Another uncertainty of the DOM data lies in the time of the aerial survey, which always took place in winter when deciduous trees are without leaves, in order to better detect the ground surface for the DEM. This results in the greater variability of heights of individual landscape elements, most especially for line elements such as hedgerows. Since this in turn is compensated by greater heights, there is no serious change in the overall assessment of wind erosion risk when considering the analysis as a whole. Thus, this analysis remains a compromise between accuracy and actuality, which, however, cannot be achieved any other way in the mapped Federal State wide scale. Years of work on this topic have shown us that even the best state-of-the-art analysis can be permanently improved, either methodically or by means of improved computing technology. Ultimately, the aim of this work was to provide a uniform assessment of the wind erosion risk for all agriculturally used soils of Brandenburg. The current state of the landscape structure model is prepared for future developments and also enables the integration of further aspects of landscape analysis with a high spatial accuracy at any scale of available data. The final query of the erosion risk with the structures of the field blocks provides the immediate answer to preferred areas on which protective measures are necessary or particularly useful. These can be integrated agronomic measures, but also the implementation of more permanent protection through windbreak hedges.

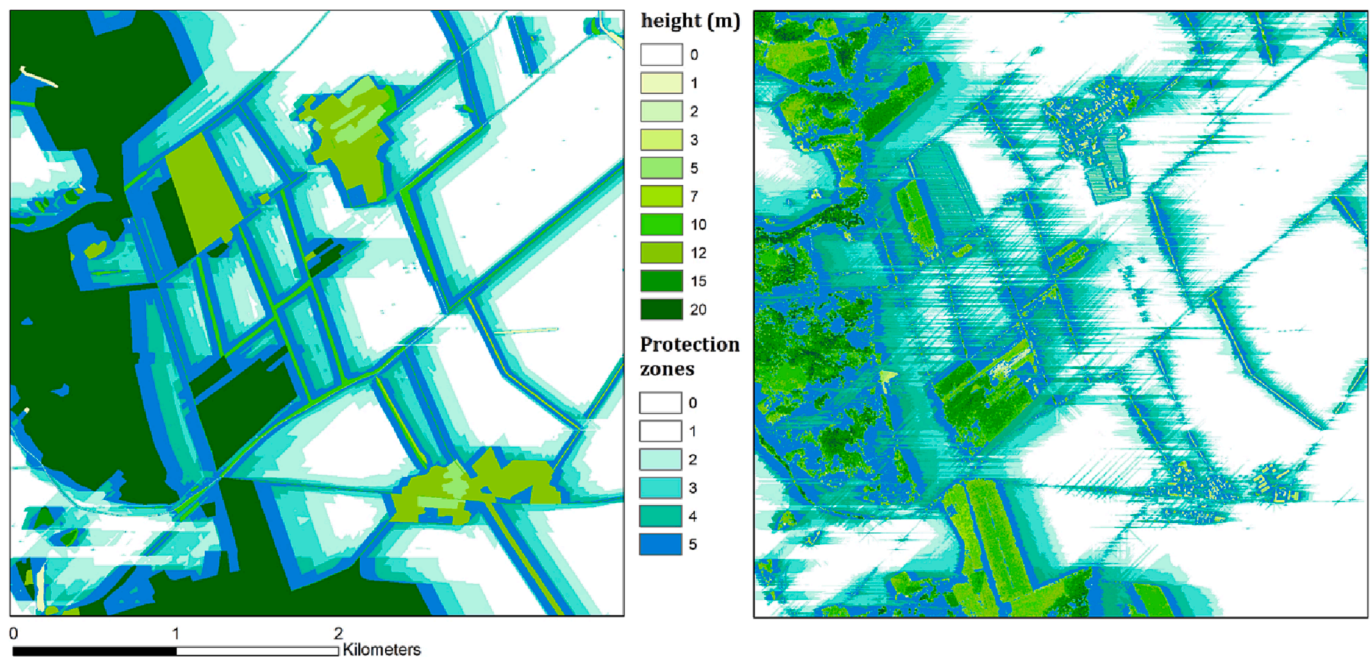


Fig. 12. Wind protective effects of all assigned (left) and measured (right) landscape elements (same map section of MOL as shown in Fig. 4).

Declaration of Competing Interest

The authors declare that they have no known competing financial interests or personal relationships that could have appeared to influence the work reported in this paper.

Data availability

Data will be made available on request.

Acknowledgements

The project was supported by the Ministry of Agriculture, Environment and Climate Protection (MLUK) of the Federal State of Brandenburg. We would like to thank Jürgen Budewitz and Jürgen Pickert from the MLUK for their advancing and constant support of the project as well as the organization of permanent exchanges with the local administrations and concerned farmers in BRB.

References

- ATKIS (2013). Amtliches Topographisch-Kartographisches Informationssystem ATKIS®, <https://geoportal.brandenburg.de>, last access: 21.10.2022.
- Bach, M., 2008. Äolische Stofftransporte in Agrarlandschaften – Experimentelle Untersuchungen und räumliche Modellierung von Bodenerosionsprozessen durch Wind (Ph.D. Thesis). University of Kiel, Germany, 129 pp.
- Baker, T.P., Moroni, M.T., Hunt, M.A., Worledge, D., Mendham, D.S., 2021. Temporal, environmental and spatial changes in the effect of windbreaks on pasture microclimate. *Agricultural and Forest Meteorology* 297, 108265. <https://doi.org/10.1016/j.agrformet.2020.108265>.
- Böhm, C., Kiesel, J., Deumlich, D., Thieme, J., 2009. An approach to extrapolate categorical agricultural soil data to nonmapped areas using majority vote. *J. Plant Nutr. Soil Sci.* 172, 467–476. <https://doi.org/10.1002/jpln.200700057>.
- Borelli, P., Balladio, C., Panagos, P., Montanarella, L., 2014. Wind erosion susceptibility of European soils. *Geoderma* 232–234, 471–478. <https://doi.org/10.1016/j.geoderma.2014.06.008>.
- Borelli, P., Lugato, E., Montanarella, L., Panagos, P., 2017. A new assessment of soil loss due to wind erosion in European agricultural soils using a quantitative spatially distributed modelling approach. *Land Degrad. Develop.* 28, 335–344. <https://doi.org/10.1002/ldr.2588>.
- Brune, M., 2016. Urban trees under climate change – Potential impacts of dry spells and heat waves in three German regions in the 2050s. Report 24. Climate Service Center Germany, Hamburg. <https://www.climate-service-center.de/imperia/md/content/csc/report24.pdf>, last access: 21.10.2022.
- Chappell, A., Heritage, G.L., 2007. Using illumination and shadow to model aerodynamic resistance and flow separation: An isotropic study. *Atmospheric Environment* 41, 5817–5830. <https://doi.org/10.1016/j.atmosenv.2007.03.037>.
- Conen, F., Leifeld, J., 2014. A new facet of soil organic matter. *Agriculture, Ecosystems and Environment* 185, 186–187. <https://doi.org/10.1016/j.agee.2013.12.024>.
- DIN 19706. Soil quality - Determination of the soil exposure risk from wind erosion. German Institute for Standardisation. Deutsches Institut für Normung e.V., Beuth Verlag GmbH, 2004.
- DWD 2004: https://www.dwd.de/DE/leistungen/windkarten/deutschland_und_bundeslaender.html, last access: 21.10.2022.
- EC 1593/2000. COUNCIL REGULATION (EC) No 1593/2000 of 17 July 2000 amending Regulation (EEC) No 3508/92 establishing an integrated administration and control system for certain Community aid schemes. <https://eur-lex.europa.eu/eli/reg/2000/1593/oj>, last access: 21.10.2022.
- Elliot, W.P., 1958. The growth of the atmospheric internal boundary layer. *Eos, Transactions American Geophysical Union* 39 (6), 1048–1054.
- Favet, J., Lapanje, A., Giongo, A., Kennedy, S., Aung, Y.-Y., Cattaneo, A., Davis-Richardson, A.G., Brown, C.T., Kort, R., Brumsack, H.-J., Schnetger, B., Chappell, A., Kroijenga, J., Beck, A., Schwibbert, K., Mohamed, A.H., Kirchner, T., de Quadros, P. D., Triplett, E.W., Broughton, W.J., Gorbushina, A.A., 2013. Microbial hitchhikers on intercontinental dust: catching a lift in Chad. *The ISME Journal* 7 (4), 850–867.
- Flood, M., 2001. LIDAR activities and research priorities in the commercial sector. *International Archives of Photogrammetry and Remote Sensing* 34, 3–7.
- Frielinghaus, M., Deumlich, D., Funk, R., Helming, K., Thieme, J., Völker, L., Winnige, B., 2002a. Beiträge zum Bodenschutz in Mecklenburg-Vorpommern, Bodenerosion. Landesamt für Umwelt, Naturschutz und Geologie, Mecklenburg-Vorpommern, Schwerin.
- Frielinghaus, M., Deumlich, D., Funk, R., Schmidt, W., Thieme, J., Völker, L., 2002b. Informationsheft zum landwirtschaftlichen Bodenschutz im Land Brandenburg, Teil Bodenerosion. Ministerium für Landwirtschaft, Umweltschutz und Raumordnung, Potsdam.
- Funk, R., Reuter, H.J., 2006. Wind Erosion in Europe. In: *Soil Erosion in Europe*. Eds.: J. Boardman and J. Poesen. Wiley, London.
- Funk, R., Engel, W., 2015. Investigations with a field wind tunnel to estimate the wind erosion risk of row crops. *Soil & Tillage Research* 145, 224–232.
- Funk, R., Deumlich, D., Steidl, J., Voelker, L., 2004b. GIS Application to Estimate the Wind Erosion Risk in the Federal State of Brandenburg. In: *Wind Erosion and Dust Dynamics*. Eds.: D. Goossens and M. Riksen. ESW Publications, Wageningen, 139–150.
- Funk, R., Skidmore, E., Hagen, L., 2004a. Comparison of wind erosion measurements in Germany with simulated soil losses by WEPS. *Environ. Modell. Softw.* 19 (2), 177–183.
- Gericke, A., Kiesel, J., Deumlich, D., Venohr, M., 2019. Recent and future changes in rainfall erosivity and implications for the soil erosion risk in Brandenburg, NE Germany. *Water* 11 (5), Article 904.
- Giongo, A., Favet, J., Lapanje, A., Gano, K.A., Kennedy, S., Davis-Richardson, A.G., Brown, C., Beck, A., Farmerie, W.G., Cattaneo, A., Crabb, D.B., Aung, Y.-Y., Kort, R., Brumsack, H.-J., Schnetger, B., Broughton, W.J., Gorbushina, A.A., Triplett, E.W., 2013. Microbial hitchhikers on intercontinental dust: high-throughput sequencing to catalogue microbes in small sand samples. *Aerobiologia* 29 (1), 71–84.

- Goossens, D., 2004. Net loss and transport of organic matter during wind erosion on loamy sandy soil. In: Goossens, D., Riksen, M. (Eds.), *Wind Erosion and Dust Dynamics: Observations, Simulations, Modelling*. ESW Publications, Wageningen, pp. 81–102.
- Goossens, D., Gross, J., 2002. Similarities and dissimilarities between the dynamics of sand and dust during wind erosion of loamy sandy soil. *Catena* 47 (4), 269–289.
- Hagen, L.E., Fox, F.A., 2020. Erosion Submodel of WEPS. In: *The Wind Erosion Prediction System (WEPS): Technical Documentation*, J. Tatarko (Ed.). USDA Agriculture Handbook 727:85-157. United States Department of Agriculture, Agricultural Research Service, Beltsville, MD.
- Hagen, L.J., Skidmore, E.L., Miller, P.L., Kipp, J.E., 1981. Simulation of the effect of wind barriers on airflow. *Transactions of the American Society of Agricultural Engineers* 24 (4), 1002–1008.
- Iturri, L.A., Funk, R., Leue, M., Sommer, M., Buschiazzo, D.E., 2017. Wind sorting affects differently the organo-mineral composition of saltating and particulate materials in contrasting texture agricultural soils. *Aeolian Research* 28, 39–49.
- LGB, 2020. Landesvermessung und Geobasisinformation Brandenburg - Digital Elevation Model of Brandenburg. <https://geobasis-bb.de/lgb/de/geodaten/3d-produkte/>, last access: 07.03.2023.
- LGB, 2023. Landesvermessung und Geobasisinformation Brandenburg - Digitales Feldblock Kataster. <https://geobroker.geobasis-bb.de/gbss.php?MODE=GetProductInformation&PRODUCTID=9e95f21f-4ecf-4682-9a44-e5f7609f6fa0>, last access: 07.03.2023.
- LGBR, 2020. Federal Service for Mining, Geology and Resources. Maps of the LBGR: <http://www.geo.brandenburg.de/lbgr/bergbau>, last access: 21.10.2022.
- Li, J., Kandakji, T., Lee, J.A., Tatarko, J., Blackwell III, J., Gill, T.E., Collins, J.D., 2018. Blowing dust and highway safety in the southwestern United States: Characteristics of dust emission “hotspots” and management implications. *Science of the Total Environment* 621, 1023–1032.
- Marshall, J.K., 1971. Drag measurements in roughness arrays of varying density and distribution. *Agricultural Meteorology* 8, 269–292.
- McEachran, A.D., Blackwell, B.R., Hanson, J.D., Wooten, K.J., Mayer, G.D., Cox, S.B., Smith, P.N., 2015. Antibiotics, bacteria, and antibiotic resistance genes: aerial transport from cattle feed yards via particulate matter. *Environ. Health Perspect.* 123 (4), 337–343.
- Mendez, M.J., Aimar, S.B., Aparicio, V.C., Haberkon, N.B.R., Buschiazzo, D.E., De Geronimo, E., Costa, J.L., 2017. Glyphosate and Aminomethylphosphonic acid (AMPA) contents in the respirable dust emitted by an agricultural soil of the central semiarid region of Argentina. *Aeolian Research* 29, 23–29.
- MLUK, 2021. Ministerium für Klimaschutz, Landwirtschaft, ländliche Räume und Umwelt. <https://www.regierung-mv.de/Landesregierung/lm/Umwelt/Boden/Boden-schutz/Gefahrdeung-des-Bodens/Erosion/>, last access: 21.10.2022.
- MLUK, 2009. CIR-Biototypen 2009 (Luftbildinterpretation) - Flächendeckende Biotop- und Landnutzungskartierung im Land Brandenburg (BTLN). <https://metaver.de/search/dls/?serviceId=473A728C-83D5-466C-A610-3278DE0F1DF5>, last access: 08.03.2023.
- Münch, S., Papke, N., Thiel, N., Nübel, U., Siller, P., Roesler, U., Biniash, O., Funk, R., Amon, T., 2020. Effects of farmyard manure application on dust emissions from arable soils. *Atmospheric Pollution Research* 11 (9), 1610–1624.
- Nägeli, W., 1941. Über die Bedeutung von Windschutzstreifen zum Schutze landwirtschaftlicher Kulturen. *Schweiz. Z. f. Forstwesen* 11, 265–280.
- Nerger, R., Funk, R., Cordsen, E., Fohrer, N., 2017. Application of a modelling approach to designate soil and soil organic carbon loss to wind erosion on long-term monitoring sites (BDF) in Northern Germany. *Aeolian Research* 25, 135–147.
- Pásztor, L., Négyesi, G., Laborczi, A., Kovács, T., László, E., Bihari, Z., 2016. Integrated spatial assessment of wind erosion risk in Hungary. *Nat. Hazards Earth Syst. Sci.* 16 (11), 2421–2432.
- Raupach, M.R., 1992. Drag and drag partition on rough surfaces. *Boundary-Layer Meteorology* 60, 374–396.
- Reich, P., Eswaran, H., Beinroth, F., 2001. Global dimensions of vulnerability to wind and water erosion. In: D.E. Scott, R.H. Mohtar and G.C. Steinhardt (eds.) 2001. *Sustaining the Global Farm. Selected papers from the 10th International Soil Conservation Organization Meeting held May 24-29, 1999 at Purdue University and the USDA-ARS National Soil Erosion Research Laboratory*, 838-846.
- Schmidt, M., Nendel, C., Funk, R., Mitchell, M., Lischeid, G., 2019. Modelling yields response to shading in the field-to-forest transition zones in heterogeneous landscapes. *Agriculture* 9, 6.
- Stackebrandt, W., Franke, D., 2015. *Geologie von Brandenburg*. Schweizerbart, Stuttgart, p. 806.
- Steinke, I., Funk, R., Busse, J., Iturri, A., Kirchen, S., Leue, M., Möhler, O., Schwartz, T., Schnaiter, M., Sierau, B., Toprak, E., Ullrich, R., Ulrich, A., Hoose, C., Leisner, T., 2016. Ice nucleation activity of agricultural soil dust aerosols from Mongolia, Argentina and Germany. *Journal of Geophysical Research: Atmospheres* 121 (22), 13559–13576.
- Sterk, G., Herrmann, L., Bationo, A., 1996. Wind-blown nutrient transport and soil productivity changes in Southwest Niger. *Land Degradation & Development* 7 (4), 325–335.
- USDA-ARS, 2020. *The Wind Erosion Prediction System (WEPS): Technical Documentation*, J. Tatarko (Ed.). USDA Agriculture Handbook 727. United States Department of Agriculture, Agricultural Research Service, Beltsville, MD. 533 pp.
- van Eimern, J., 1964. Untersuchungen über das Klima in Pflanzenbeständen als Grundlage einer agrarmeteorologischen Beratung, insbesondere für den Pflanzenschutz. *Berichte des Deutschen Wetterdienstes* 96, 76 pp.
- Vigjak, O., Sterk, G., Warren, A., Hagen, L.J., 2003. Spatial modeling of wind speed around windbreaks. *Catena* 52 (3-4), 273–288.
- Ziegler, N. P., Webb, N. P., Chappell, A., LeGrand, S. L., 2020. Scale invariance of albedo-based wind friction velocity. *Journal of Geophysical Research: Atmospheres*, 125, e2019JD031978. <https://doi.org/10.1029/2019JD031978>.
- Zolina, O., Simmer, C., Belyaev, K., Gulev, S.K., Koltermann, P., 2013. Changes in the Duration of European Wet and Dry Spells during the Last 60 Years. *J. Clim.* 26, 2022–2047.